13th International Conference on
Structural Health Monitoring of Intelligent Infrastructure
DOI: 10.3217/978-3-99161-057-1-196

Multi-scale digital twin for a high-rise structure combining ANN and monitoring data

Hetian Shao[1], Wei Lu[1], Wenchang Zheng[1], Weihua Hu[1], Jun Teng[1], Eric M. Lui[2]
[1]School of Intelligent Civil and Ocean Engineering, Harbin Institute of Technology, 518055 Shenzhen, China
[2]Department of Civil & Environmental Engineering, Syracuse University, Syracuse, NY 13244-1240, USA
email: hetianshao@stu.hit.edu.cn, lu.wei@hit.edu.cn, 23s054026@stu.hit.edu.cn,
huweihua@hit.edu.cn, tengj@hit.edu.cn, emlui@syr.edu

ABSTRACT: The application of digital twin technology in high-rise buildings provides a comprehensive approach to maintaining construction safety, tracking project advancement, and evaluating service conditions. This paper proposes a novel multi-scale digital twin framework for high-rise structures. The macro-scale model is constructed using spring elements, taking into account the dynamic behavior of flexure-shear coupling in high-rise structures. The macro-scale digital twinning is achieved by updating the macro-scale model through the integration of modal monitoring data with Artificial Neural Networks (ANN). A multi-scale analysis method from the structural macro-level to components of the substructure is developed through information transfer at boundary nodes, achieving a balance between computational efficiency and the demand for accuracy of the local components. Integrated with multiple monitoring data sources, the proposed framework provides a technical pathway for multi-scale model updating, real-time response acquisition, and disaster risk assessment of high-rise structures.

KEY WORDS: High-rise building; Flexure-shear coupled behavior; Multi-scale analysis; Structural health monitoring; Artificial Neural Networks.

1 INTRODUCTION

Digital twins are increasingly recognized as pivotal innovations within the Architecture, Engineering, Construction, and Facility Management (AEC-FM) industry [1,2]. As an advanced representation that bridges the digital and physical realms, digital twins enable researchers and practitioners to gain a more intuitive and in-depth understanding of the real-time state and operational principles of objects.

Incorporating mechanical information of the structure into the building's digital twin can provide an approach to maintaining construction safety, tracking project advancement, and evaluating service conditions. Typically, modal monitoring data of the building is used to correct the parameters of the structural design model [3,4]. The advantage lies in the maturity and convenience of the monitoring methods, and the structural design model can be detailed to the component level, offering a high degree of adjustability. However, the computational efficiency of the design model is low, and model updating typically requires a large number of iterative calculations or reference samples.

The updating of macro-scale models is a very promising research direction, aimed at improving the efficiency of model updating while fully utilizing structural modal monitoring data [5,6]. However, the coupling effects of bending and shear in high-rise structures as well as the complex inter-story force distribution can significantly affect the dynamic characteristics of macro-scale models. The mapping of macro-scale characteristics to model updating through modal monitoring data is also significantly influenced by the identification algorithms [7,8]. Therefore, researching suitable macro-scale model carriers and model updating algorithms are the two main research directions in the identification of macro-scale models.

Macro-scale models can only represent the overall deformation of the structure and cannot delve into the load-bearing status of local components. There are certain special components and critical load-bearing areas where there is a higher demand for monitoring and digital twin accuracy. To balance computational efficiency and simulation precision, a multi-scale structural model is an ideal research approach [9,10]. Information transfer or coupling between different scales is key to implementing this technology. The multi-scale twin model that combines macro-scale models with component-scale substructure models is still an area that requires further research.

This paper proposes a multi-scale digital twin method that integrates both macro-scale and component-scale substructures. First, a macro-scale twin is realized through Artificial Neural Networks (ANN) and modal monitoring data, and then a substructure component-scale twin is achieved by constructing a floor boundary condition transmitter. Integrated with multiple monitoring data sources, the proposed framework provides a technical pathway for multi-scale model updating, real-time response acquisition, and disaster risk assessment of high-rise structures.

2 MACRO-SCALE MODEL UPDATING

2.1 *Floor deformation characterization*

Story response is often used to quantify the overall behavior of high-rise buildings. Therefore, the primary focus is on the displacements of the floor boundary nodes to represent the overall deformation situation of the high-rise buildings. Characterizing the displacements of the numerous boundary nodes on each floor is key to building a macro-scale model of high-rise structures.

In this paper, a high-rise frame core tube structure shown in Figure 1a is used as an example, The structure has 40 stories, each with a height of 4.0 meters. The columns and beams were

DOI: 10.3217/978-3-99161-057-1-196

modeled using Euler-Bernoulli beam elements, and the core wall was modeled using shell elements. To simplify the complexity of constructing the macro-scale models, uniform member sizes and materials were adopted for all structural components. All columns were 800×800 mm² rectangular C40-RC columns and all beams were 500×1000 mm² rectangular C30-RC beams, except for the coupling beams in the core wall, which have a cross-section of 700×1400 mm². The material properties are: C30 concrete ($E = 3.0\times10^7$ kN/m², $\nu = 0.25$, $\rho = 25$ kN/m³) and C40 concrete ($E = 3.25\times10^7$ kN/m², with ν and ρ assumed identical to C30). The wall thickness of the core tube is 900 mm. This model also incorporates simplified simulations of infill walls, exterior curtain walls, and rigid panel zones, which, due to space limitations, are not discussed in detail in this paper. However, these structural details significantly increase the computational demands and time costs of the model. The multi-scale modeling approach proposed in this study is specifically designed to optimize this issue.

The structural analysis software OpenSees was used to model the structure (shown in Figure 1b) for batch extraction of the deformation of nodes. Modal analysis of the structure was performed (shown in Figure 2) under the assumption that deformations are restricted to the x-direction, with rigid constraints applied in the other two directions.

The deformation of the planes where the floor boundary nodes are located is illustrated in Figure 3. Due to the rigid floor assumption, the horizontal displacement is uniform at all points, while the vertical deformation and torsional deformation vary from point to point. Therefore, it is proposed to use two hypothetical planes to represent the overall situations of vertical displacement and torsional displacement, respectively. The vertical displacement of each node was fitted to a Hypothetical Vertical Displacement Plane (HVDP) using the least squares method. The bending deformation of the nodes in each slab was averaged to form a Hypothetical Bending Displacement Plane (HBDP). The angle of rotation of HBDP (α_{HBDPi} for the i^{th} floor) and HVDP (β_{HVDPi} for the i^{th} floor) shown in Figure 3 represents their degree of displacement. For a given mode, the vertical and bending modal vectors of the boundary nodes of each story were fitted to an HVDP and HBDP, respectively. Examples of this fitting for the 1st floor of the 1st mode are given in Figure 4. Examples of the angles of the HBDPs and the HVDPs of the 1st and 2nd modes were calculated and shown in Figure 5.

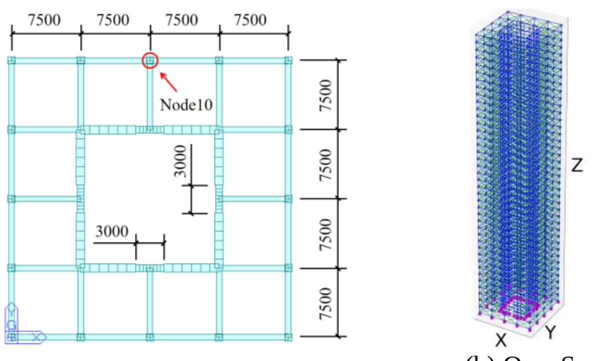

(a) Story plan

(b) OpenSees model

Figure 1. High-rise frame core tube structure.

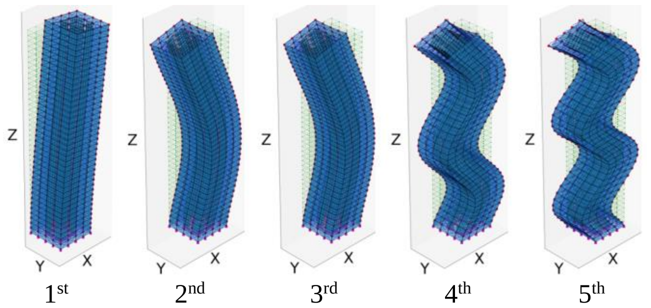

Figure 2. Mode shapes of the high-rise frame core tube structure.

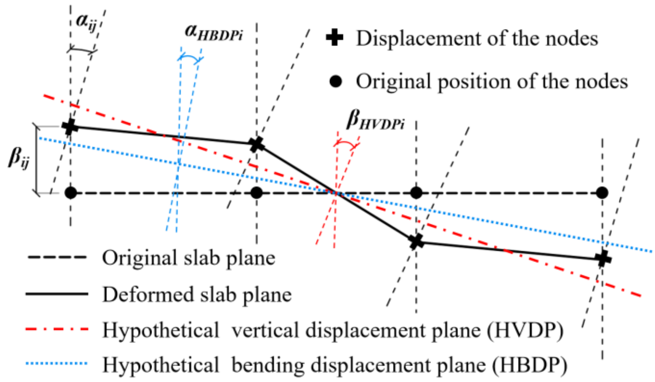

Figure 3. Displacements of the story nodes.

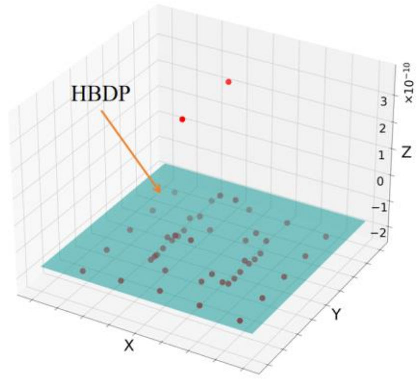

(a) HBDP

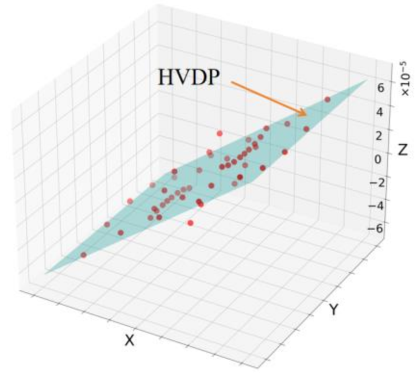

(b) HVDP

Figure 4. Hypothetical plane of the 1st mode of the 1st floor.

DOI: 10.3217/978-3-99161-057-1-196

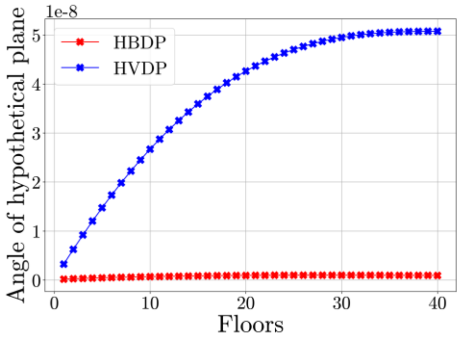

(a) 1st mode

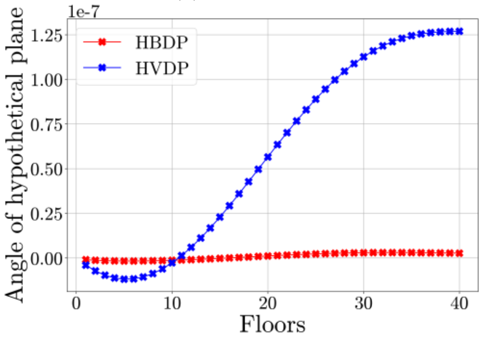

(b) 2nd mode

Figure 5. HBDP and HVDP

HBPV offers a way to isolate the displacement components induced by bending. The displacement Δ_{Bi} induced by bending for the i^{th} floor can be approximated by the equation

$$\Delta_{Bi} = (\tan\varphi + \lambda\tan\omega)H_i \tag{1}$$

where φ is the angle of HBDP of the story below; ω is the change in angle of HBDP of the story; H_i is the height of the story; and λ is a correction coefficient (set as 0.5 in the present study).

The displacement induced by shear Δ_{Si} for the i^{th} floor can be calculated as

$$\Delta_{Si} = \Delta_{Ti} - \sum_{i=1}^{N}\Delta_{Bi} \tag{2}$$

where Δ_{Ti} is the lateral displacement, and N is the total number of floors.

Two normalized difference parameters D_{VBi} and D_{BTi} are defined to represent the relationship of the boundary nodes.

$$D_{VBi} = \frac{N(\alpha_{HBDPi} - \beta_{HVDPi})}{\sum_{i=1}^{N}\left(|\alpha_{HBDPi}| + |\alpha_{HBDPi}|\right)} \tag{3}$$

$$D_{BTi} = \frac{N(\Delta_{Ti} - \Delta_{Bi})}{\sum_{i=1}^{N}\left(|\Delta_{Ti}| + |\Delta_{Bi}|\right)} \tag{4}$$

The introduction of these two hypothetical planes, along with the two normalized difference parameters, provides the theoretical foundation for the subsequent updating of the macro-scale model.

2.2 Model construction and recognition

To account for the coupling of bending and shear in high-rise structures, a macro-scale model framework was constructed using spring elements, as shown in Figure 6. Each floor is composed of four identical vertical members, two identical outside horizontal members, and one inside horizontal member. Spring elements that represent the axial, shear, and bending stiffnesses of each member are shown in Figure 7. The 6×6 member stiffness matrix relating the axial, transverse, and rotational degrees-of-freedom for each node of the 2-node member with spring elements is given in Equation (5) and (6).

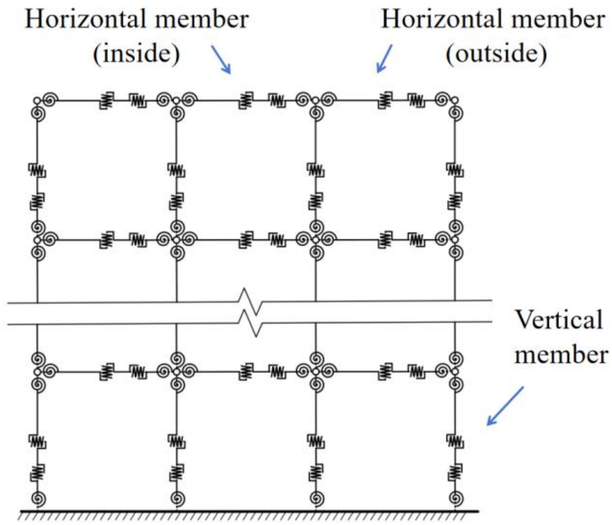

Figure 6. Macro-scale model of the high-rise structure.

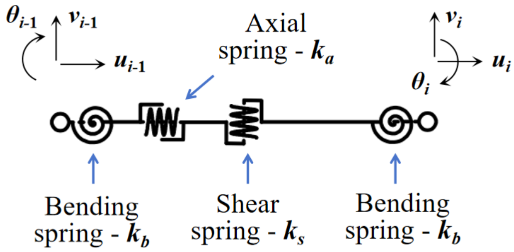

Figure 7. Member with springs

$$\frac{1}{\eta}\begin{pmatrix} k_a\eta & & & & & \text{sym.} \\ & 2k_bk_s & & & & \\ & k_bk_sl & k_b^2+k_bk_sl^2 & & & \\ -k_a\eta & & & k_a\eta & & \\ & -2k_bk_s & -k_bk_sl & & 2k_bk_s & \\ & k_bk_sl & -k_b^2 & & -k_bk_sl & k_b^2+k_bk_sl^2 \end{pmatrix} \tag{5}$$

$$\eta = 2k_b + k_sl^2 \tag{6}$$

DOI: 10.3217/978-3-99161-057-1-196

The macro-scale model of the typical 40-story frame core tube structure is constructed using ANN and simulated modal monitoring data. As shown in Figure 8, natural frequencies, lateral mode vectors, angular mode vectors of the HBDP, D_{VB} and D_{BT} were selected as the features. The stiffness of the springs was the target to be recognized, i.e., a total of 7 stiffness coefficients (k_a, k_b, k_s, k_{hb}, k_{hs}, k_{ihb} and k_{ihs}). k_a is the axial stiffness, k_b and k_s are the bending and shear stiffness of the column, k_{hb} and k_{hs} are the bending and shear stiffness of the outside horizontal members, while k_{ihb} and k_{ihs} are the bending and shear stiffness of the inside horizontal members. The initial values of the stiffness parameters were roughly estimated through a small number of trial calculations, as shown in Table 1. 20000 samples were generated through Latin square sampling with the combination of different stiffness change ranges as shown in Table 2 and batch modal analysis. A type of ANN that is conducive to utilizing the spatial information between data, Convolutional Neural Networks (CNN) incorporating channel and spatial attention mechanisms (CBAM-CNN) [11] were used, and a (non-learnable) Fixed attention layer (FixAL) was selectively added to manually assign weights to different features [12]. The specific network architecture and hyperparameter settings of the ANN are shown in

Table 3 and Table 4, respectively.

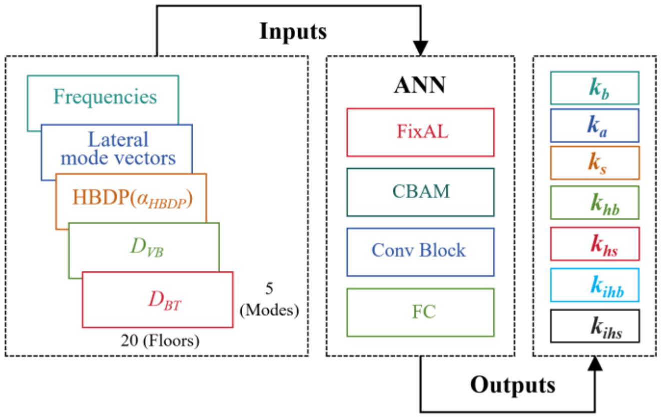

Figure 8. ANN model construction.

Table 1. Stiffness parameters

Stiffness	Initial	Recognized
k_a	7.00×10^{7}	6.92×10^{7}
k_b	1.50×10^{14}	1.58×10^{14}
k_s	1.00×10^{12}	9.87×10^{11}
k_{hb}	8.00×10^{13}	7.90×10^{13}
k_{hs}	1.00×10^{14}	9.87×10^{13}
k_{ihb}	4.00×10^{13}	3.94×10^{13}
k_{ihs}	1.00×10^{14}	$9.88\text{e}\times10^{13}$

The units of k_s, k_a, k_{hs}, k_{ihs} are N/mm; and the units of k_b, k_{hb}, k_{ihb} are N-mm/rad

Table 2. Sample set stiffness variation ranges

Dataset	Variation ranges (%)	Size
1	(80-120)	10000
2	(90-110)	10000

Table 3. The main structure of the ANN

Layer	Type	Output size[a]
Input	Modal data	bs×1×5×5×40
FixAL[b]	Weight matrix-1	bs×1×5×5×40
	Weight matrix-2	bs×1×5×5×40
CB[c]	Conv3d	bs×16×5×5×40
	ReLU	-
	Max pooling	bs×16×2×2×20
CB	Conv3d	bs×32×2×2×20
	ReLU	-
	Max pooling	bs×32×2×2×10
CB	Conv3d	bs×64×2×2×10
	ReLU	-
	Max pooling	bs×64×1×1×5
CBAM[d]	Channel attention	bs×64×1×1×5
	Spatial attention	bs×64×1×1×5
DL[e]	-	-
FC[f]	Flatten	bs×320
	FC cells	bs×320
	ReLU	-
	FC cells	bs×1000
	ReLU	-
	FC cells	bs×256
Output	Stiffness parameters	bs×7

[a] bs = batch size; [b] FixAL = Fixed Attention Layer; [c] CB = Convolutional Block; [d] CBAM = Convolutional Block Attention Module; [e] DL = Dropout Layer; [f] FC = Fully Connected Layer

Table 4. Hyperparameter settings of the ANN

Parameters	Value
Number of epochs	50
Batch size	256
Learning rate	0.0001-0.00001
Kernel size of Conv3d	3×3×3
Weight decay (L2 regularization)	1.0e-3
Dropout rate	0.2

The learning curve is shown in Figure 9, and the recognized stiffness parameters with the developed ANN model are shown in Table 1. With the recognized stiffness parameters, the macro-scale model of the typical high-rise frame core tube building was constructed. The modal analysis of the macro-scale model was carried out as shown in Figure 10. Comparison of the dynamic characteristics of the macro-scale model and original full-order model is shown in Table 5, Figure 11, Figure 11 and Figure 12. It is evident that the recognized model provides a good fit for the macro-scale mechanical properties of the original full-order model.

DOI: 10.3217/978-3-99161-057-1-196

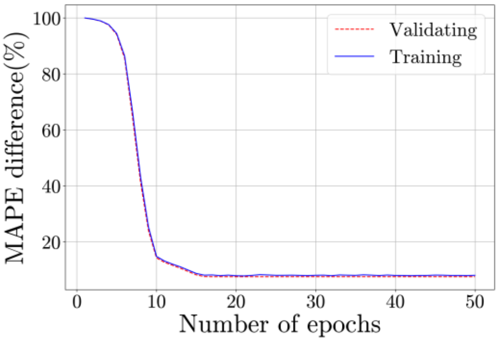

Figure 9. Maximum Absolute Percent Error (MAPE) difference.

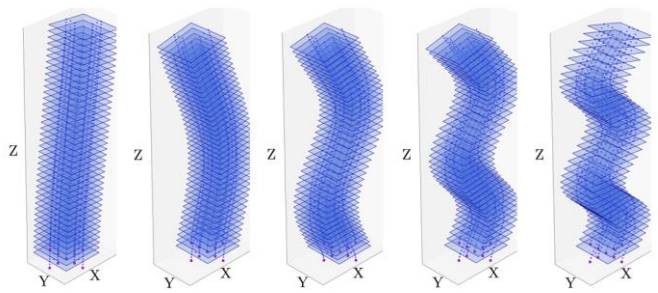

(a) 1st (b) 2nd (c) 3rd (d) 4th (e) 5th

Figure 10. Mode shapes of the recognized macro-scale model.

Table 5. Comparison of the dynamic characteristics

Mode	Frequency (Hz)			MAC (%)	HBDP MAC (%)
	Original model	Recognized model	Difference (%)		
1	0.35	0.36	-2.15	1.000	0.9997
2	1.43	1.46	-2.15	0.9999	0.9978
3	3.00	2.97	1.02	0.9999	0.9986
4	4.67	4.67	0.11	0.9999	0.9986
5	6.54	6.55	-0.17	0.9996	0.9884

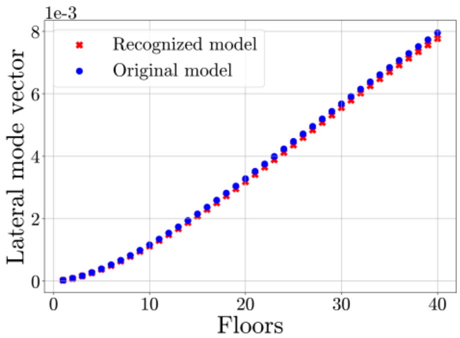

(a) 1st mode

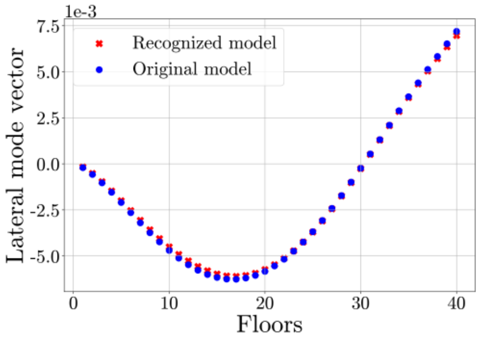

(b) 2nd mode

Figure 11. Lateral mode vectors of the models.

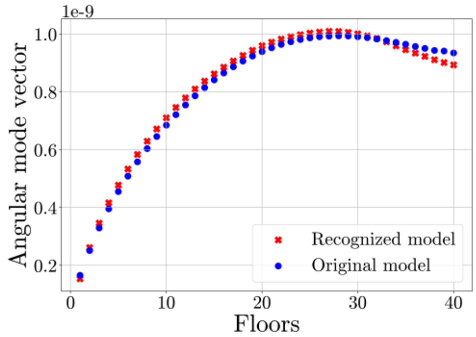

(a) 1st mode

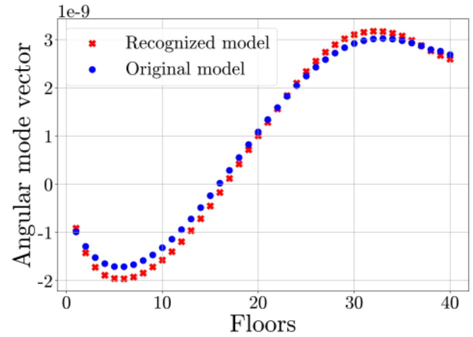

(b) 2nd mode

Figure 12. HBDP angles of the models.

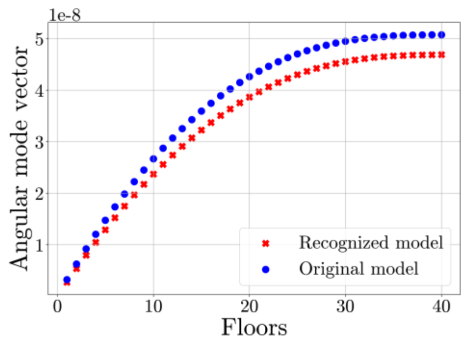

(a) 1st mode

DOI: 10.3217/978-3-99161-057-1-196

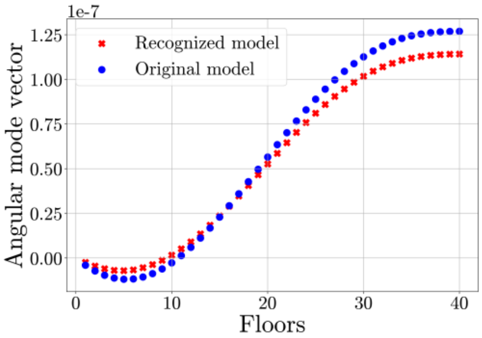

(b) 2nd mode

Figure 13. HVDP angles of the models.

3 MULTI-SCALE DIGITAL TWIN

3.1 Multi-scale model

The macro-scale model proposed above can only analyze the structural response at the overall level of each floor. However, for certain special structural components or critical load-bearing areas, it is desirable to analyze the structural response of specific components.

Based on the proposed macro-scale model, this paper employs the transmission of boundary condition information to perform structural response calculations at the component level for substructures, thereby achieving multi-scale digital twins. The key to the method lies in constructing a boundary condition transmitter, as shown in Figure 14, which can expand and map the macro-scale deformation of a certain floor to the deformation of each boundary node on that floor. This paper constructs the boundary condition transmitter using the proposed HBDP, HVDP, and the proportional relationships of the modal vectors corresponding to each floor's boundary nodes under their first-order modes, as shown in Equations (7), and (8).

$$\Delta_{Bi} = \alpha_{HBDPi} M_{Bi} \tag{7}$$

$$\Delta_{Vi} = \beta_{HVDPi} M_{Vi} \tag{8}$$

where Δ_{Bi} and Δ_{Vi} are the bending and vertical displacements of the i^{th} node of the story in question, respectively; M_{bi} and M_{vi} are the displacements of the i^{th} node of the story in question per unit angle of α_{HBDPi} and β_{HVDPi}, respectively.

The lateral displacement of each node is consistent with the lateral displacement of the macro-scale model. Using the displacements of the macro-scale model to map the displacements of the boundary nodes of the substructure model, the substructure's deformation can now be realized. The construction of the boundary condition transmitter can be refined according to the requirements, and can even further consider the coupling relationship between displacements of different degrees of freedom, which will be a subject of further research.

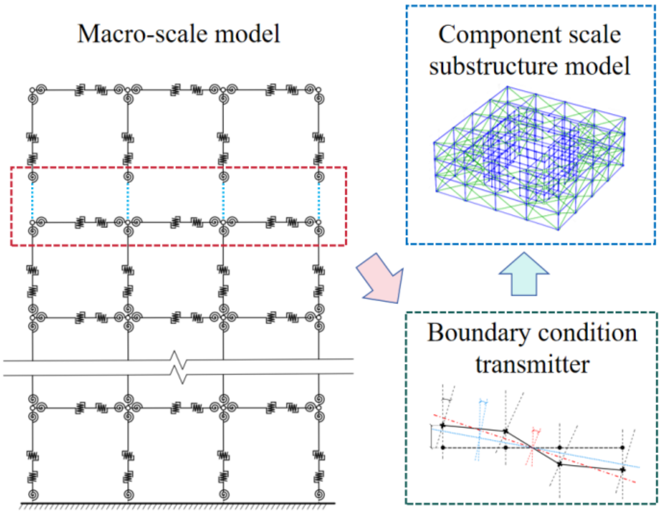

Figure 14. Deformation transfer from boundary nodes to the substructure.

3.2 Substructural response

To verify the feasibility and accuracy of the proposed multi-scale model, the 20th and 21st floors of the high-rise frame core tube structure were selected as the objects of study. The mapping relationship M_{B19}, M_{V19} and M_{B21}, M_{V21} were established and the substructure model of the 20th and 21st floors was built. A static analysis was employed for an initial attempt (as shown in Figure 15a), specifically by applying a 1000 kN force in the horizontal direction on the topmost floor of the macro-scale model. The lateral deformations and HBDP and HVDP angles of the 19th and 21st floors were calculated. Subsequently, the displacements of the boundary nodes of the substructure were calculated using Equations (7) and (8) and applied to the substructure. The deformations of the substructure were further calculated and are depicted in Figure 16.

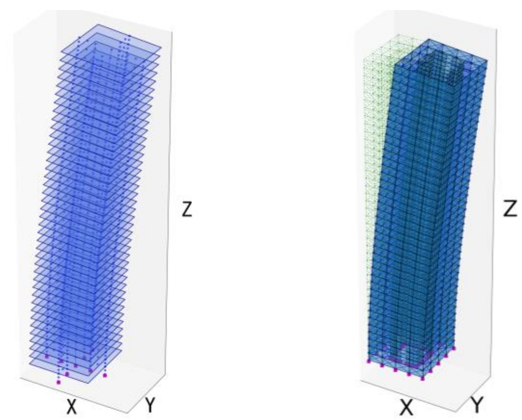

(a) Macro-scale model (b) Original model

Figure 15. Deformation of the models.

DOI: 10.3217/978-3-99161-057-1-196

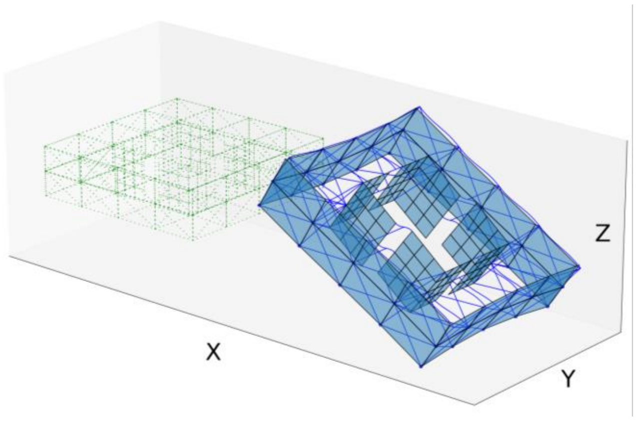

Figure 16. Deformation of the substructure (magnified).

For reference, a static analysis was performed on the original full-order model under the same loading condition. Meanwhile, the displacements of all nodes on the 20th floor for each degree of freedom were extracted from both the original full-order model and the substructure model for comparative study. Their absolute mean values and relative errors are shown in Table 6. The results show that the lateral displacement exhibits good agreement, while certain discrepancies exist in the vertical and torsional displacements. This is because the applied load distribution differs from the inertial force distribution during structural vibration.

Table 6. Comparison of the static deformation of the models

DOF	Absolute mean deformation		Error (%)
	Original model	Substructure model	
Lateral (mm)	4.40	4.54	3.26
Vertical (mm)	0.55	0.45	20.63
Torsional (rad)	9.03e-05	7.10e-05	21.40

Incremental dynamic analyses were then conducted on both the original full-order model and the multi-scale model by applying the north-south component of the El Centro seismic wave with a total duration of 20 seconds. A Rayleigh damping ratio of 0.05 was assigned to the first five modes of the structures. Table 7 presents the absolute mean values and relative errors of time-history displacements for all degrees of freedom (DOF) at the 20th-floor nodes. Taking Node 10 on the 20th floor (shown in Figure 1) as an example, Figure 17 presents a comparison of time-history displacements for three degrees of freedom. As can be observed, the substructure model can effectively replicate the deformation characteristics of the full-order model. Some frequency shifts occur in the terminal vibration phase due to the minor omission of frequencies in the macro-scale model, as well as the accumulation over multiple cycles.

Notably, the multi-scale model's dynamic analysis required only 20 minutes of computational time (16 minutes for macro-scale model and 4 minutes for substructure model), significantly less than the full-scale model's 27 hours and 12 minutes under identical hardware configuration, achieving a balance between computational efficiency and the demand for accuracy of the local components.

Table 7. Comparison of the dynamic deformation of the models

DOF	Absolute mean displacement		Error (%)
	Original model	Substructure model	
Lateral (mm)	4.23	4.43	4.58
Vertical (mm)	0.43	0.40	-7.23
Torsional (rad)	7.29e-05	7.27e-05	-0.36

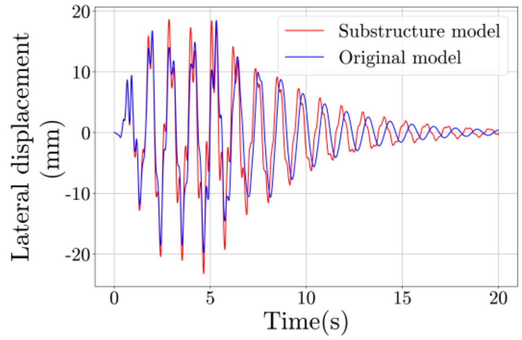

(a) Lateral displacement

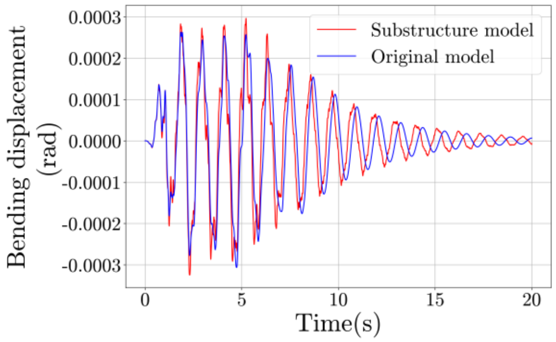

(b) Bending displacement

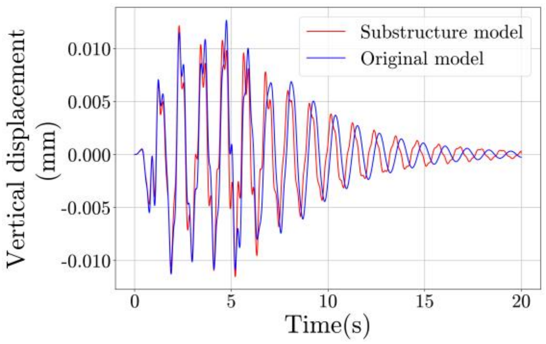

(c) Vertical displacement

Figure 17. Time-history displacements of Node 10 on the 20th floor

DOI: 10.3217/978-3-99161-057-1-196

4 CONCLUSION

This paper proposes a multi-scale digital twin method for high-rise structures. Taking a high-rise frame core tube structure as an example, a macro-scale model of the high-rise structure was constructed using a combination of spring elements, considering the coupling of bending and shear as well as the impact of the horizontal members on the structure. The macro-scale model was updated by combining Artificial Neural Networks (ANN) and modal monitoring data. Furthermore, an information transmitter was constructed using a linear mapping method to transfer the deformation from the macro-scale to the boundary nodes of the substructure at the story level, thereby enabling the calculation of deformations at the component scale of the substructure. The multi-scale digital twin method for high-rise buildings established in this study not only improves the efficiency of model updating and computation, but also meets the need for high-precision computation of local components.

ACKNOWLEDGMENTS

This work was supported by the National Key Research and Development Program of China [grant numbers 2024YFC3810504], National Natural Science Foundation of China [grant numbers 52122804, 52438004, 52378296], and the Fundamental Research Project of Shenzhen Science and Technology Plan [grant number JCYJ20220531095013030].

REFERENCES

[1] Hosamo HH, Imran A, Cardenas-Cartagena J, Svennevig PR, Svidt K, Nielsen HK. A review of the digital twin technology in the AEC-FM industry. Adv Civ Eng 2022;2022(1):2185170.
[2] Park J, Lee JK, Son MJ, Yu C, Lee J, Kim S. Unlocking the potential of digital twins in construction: a systematic and quantitative review using text mining. Buildings 2024;14(3):702.
[3] Ierimonti L, Venanzi I, Cavalagli N, Comodini F, Ubertini F. An innovative continuous Bayesian model updating method for base-isolated RC buildings using vibration monitoring data. Mech Syst Signal Process 2020;139:106600.
[4] Nguyen A, Kodikara K ATL, Chan THT, Thambiratnam DP. Deterioration assessment of buildings using an improved hybrid model updating approach and long-term health monitoring data. Struct Health Monit 2019;18(1):5-19.
[5] Lam HF, Hu J, Adeagbo MO. Bayesian model updating of a 20-story office building utilizing operational modal analysis results. Adv Struct Eng 2019;22(16):3385-3394.
[6] Prabakaran K, Kumar A, Thakkar SK. Comparison of eigensensitivity and ANN based methods in model updating of an eight-story building. Earthq Eng Eng Vib 2015;14:453-464.
[7] Behmanesh I, Moaveni B, Lombaert G, Papadimitriou C. Hierarchical Bayesian model updating for structural identification. Mech Syst Signal Process 2015;64:360-376.
[8] Akhlaghi MM, Bose S, Mohammadi ME, Moaveni B, Stavridis A, Wood RL. Post-earthquake damage identification of an RC school building in Nepal using ambient vibration and point cloud data. Eng Struct 2021;227:111413.
[9] Wang FY, Xu YL, Qu W L. Mixed-dimensional finite element coupling for structural multi-scale simulation. Finite Elem Anal Des 2014;92:12-25.
[10] Yue J, Qian J, Lei T, Lu L, Lu X. In situ lateral-loading test and micro–macro-scale simulation of an existing RC frame. Soil Dyn Earthq Eng 2013;45:35-44.
[11] Woo S, Park J, Lee JY, Kweon IS. Cbam: Convolutional block attention module, in: Proceedings of the European conference on computer vision (ECCV).3-19;2018.
[12] Zhang L, Cosmo L, Minello G, Torsello A, Rossi L. GraFix: A graph transformer with fixed attention based on the wl kernel, in: International conference on pattern recognition. Cham: Springer Nature Switzerland,15304:435-450;2024.